

## Theoretical Investigation of a Gearless Differential

*Gentcho Stainov*

*Central Laboratory of Mechatronics and Instrumentation, 1113 Sofia,  
E-mail: gentcho@clmi.bas.bg*

### 1. Introduction

Since the differential mechanisms possess two degrees of freedom, two constraints are necessary for determination of the mechanism. In the vehicle, the first constraint is the motor, and the second constraint is the frictional kinematics chain between the two wheels through the ground. Depending on the cohesion of the wheels with the ground the second constraint may become undetermined or fully disappear. The differential becomes also undetermined and transmits less or no power. For control and recovering of the second constraint various “limited slip” and “torque sensitive” differentials are used. The inner friction of some gearless differentials depends on the torque biasing that makes them “torque sensitive”, “torque-direction sensitive” and “limited slip”.

The basic theory of the differential mechanisms and analysis of various types of differentials and their calculation are presented by J a s k e v i c h [1] and L o o m a n [2]. M a d h a v a n, T s a i [3], implemented the method of “separation of structure from function” suggesting systematic methodological approach for the Mechanisms for Reverse the Direction of Rotation (MRDR) for symmetrical gearless differentials. In the enumeration, mechanisms with symmetry about the plane bisecting the shaft axes are considered.

A theoretical analysis based on the function of each of the two degrees of freedom of the differential is presented in the publications [2-5]. It is shown that all gearless differentials meet the same structure as the conventional ones. The structural scheme of the symmetrical differential is presented in Fig. 1.

The power of the motor is transmitted by the balance link without any losses through the first degree of freedom dividing the input moment. When one of the reactive moments on the outputs is smaller than  $(1/2)M_p$ , the differential effect is obtained by the circulation of the power through the second degree of freedom of the differential. Thus the properties of the differential mechanism depend on the chosen MRDR which

ensures the second degree of freedom of the differential. This mechanism could be gear, cam, and screw or lever mechanism.

The conditions for generating of MRDR and gearless differentials using Mechanisms for Converting the Rotary motion into Reciprocating motion (MCRR) are described in [3]. Depending on the possible axes of motion of the joint and the possible combinations of the reciprocating motions, the conditions for evenness and oddness of the transmission function of the MCRR mechanisms are defined. In the paper cam and lever-type gearless differentials as “Colotty” and “Ricardo” are analysed.

The MCRR mechanism could possess various friction characteristics in either directions, or moment (or velocity)-dependent friction, so the differential could be “Passive Limited Slip”.

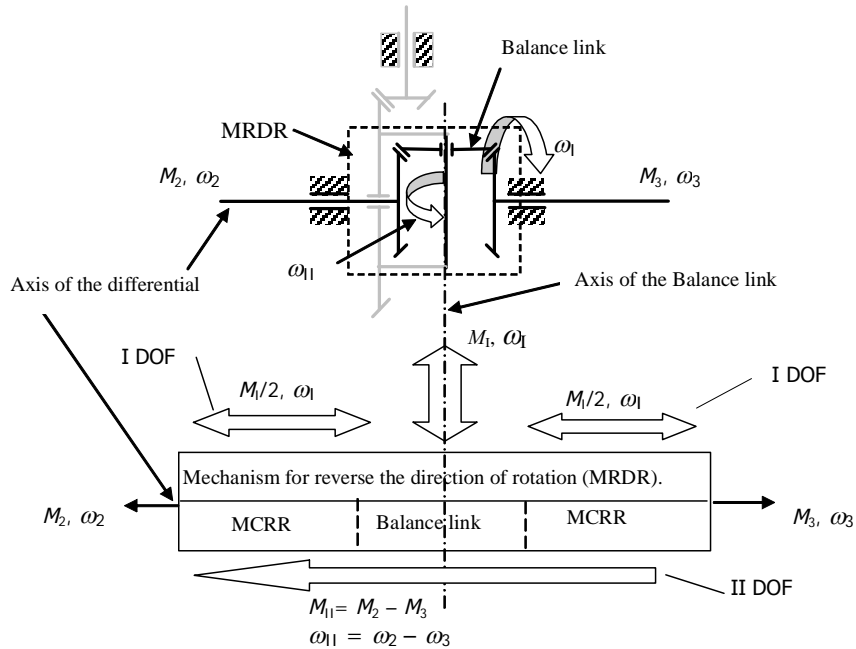


Fig. 1. Structure of the mechanism for reversing the direction of rotation and power transmission through the I and the II degrees of freedom in symmetrical differential:

I – the input moment  $M_I$  is equally distributed to the output links 2 and 3 through the I DOF of the balance link;

II – When the output power to the output links 2 and 3 is different from that distributed by I DOF, a circulation of the power  $M_{II}, \omega_{II}$  through II DOF is appearing. MCRR – Mechanisms for Converting the Rotary motion into Reciprocating motion

### Notations

- $M_{ab}$  – driving moment;
- $M_a$  – reactive moment for output  $a$ ;
- $M_b$  – reactive moment for output  $b$ ;
- $\Delta M$  – change of the moment during the operation of the differential;
- $F_{ab}$  – force on the ball from the wall of the groove;
- $F_a$  – force on the ball from the wall of the groove of the disk  $a$ , connected to output  $a$ ;
- $F_b$  – force on the ball from the wall of the groove of the disk  $b$ , connected to output  $b$ ;

$M_{\text{ball}}$  – mass of the ball;  
 $a$  – acceleration of the ball;  
 $\eta$  – coefficient for unevenness of the forces on the balls;  
 $\alpha_1, \alpha_2$  – angles of force transmission between the groves and the ball in plane  $xOy$ . (They corresponded to the angles between the tangents to the walls of the wave formed groves in the disks; for symmetrical differentials the numbers of waves of the groves on the two disks are equal and when the power is transmitted from the motor to the wheels  $\alpha_1 = \alpha_2$ );  
 $\beta_1, \beta_2$  – angles of force transmission between the groves and the ball in plane  $zOy$ ;  
 $\beta_3$  – angle of reaction force on the separator in plane  $xOz$ ;  
 $\delta$  – average axial backlash between the balls and the grooves into disks  $a$  and  $b$ ;  
 $h$  – thickness of the disks of the separator;  
 $k$  – number of simultaneously loaded balls, equal to the number of grooves in the separator;  
 $i$  – number of the waves of the groves in the disks;  
 $R_m$  – average radius of the groves in the disks;  
 $d$  – amplitude of the axle of the grooves;  
 $r$  – radius of the ball.

## 2. Description of the differential

The differential consists of two output links (first and second) and an input link formed as a separator. The first output link at the end is formed as a disk situated inside the separator. In the both sides of the disk are formed two sinusoidal groves with phase shift  $\pi$ . It allows the groves in the both disks of the separator to be coaxial. The second output link is formed as two disks situated at the both sides of the separator. The balancing links of the differential are balls oscillating in groves formed in the input and the two output links. The kinematical scheme and the disassembled parts of the differential are shown in Fig. 2.

Each ball is in contact with the radial grove of the input link (separator) and with the wave formed groves of the two output links (disks) (Fig.4). The wave formed groves of the two output links are polar sinusoids. When the separator is fixed, the two output links rotate at opposite directions and the balls oscillate into the radial groves. While the ball is in the middle part of the radial groves the sinusoidal groves are phase shifted by about  $\pi$  so that both sides of each ball are in contact with groves with equal but opposite inclination (Fig. 4).

The axle of the groves of the two output links is polar sinusoid with period  $\pi/3$  (6 periods for 1 turn).

## 3. Analysis of the differential mechanisms

The analysis is performed according to the theoretical dependences obtained in [6]. The Mechanisms for Converting the Rotary motion into Reciprocating motion (MCRR's) are of cam-type. The balance link is a ball. The rotational axis of the differential is  $z$  and the reciprocating movement of each of the balance links is along the axis perpendicular to the  $z$  axis (case A1).

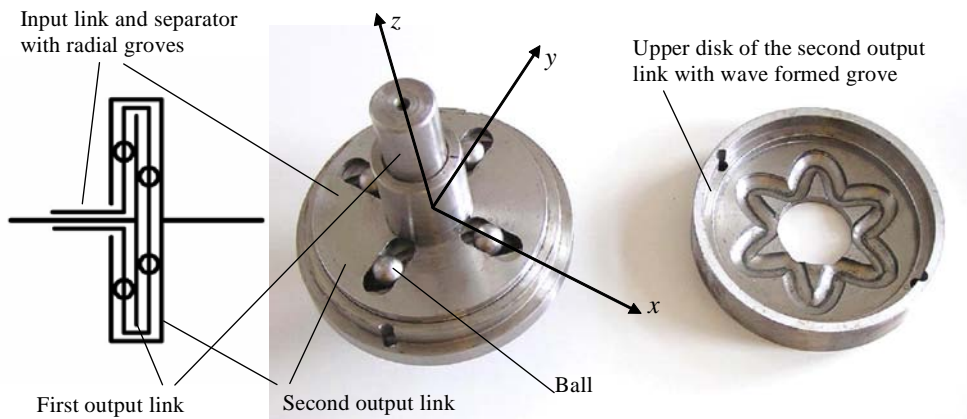


Fig. 2. Kinematical scheme and disassembled view of the differential

The elementary cam MCRR consists of a ball situated symmetrically to the groove of the separator and contacted to the groove of one of the output disk.

The Mechanism for reversing the direction of rotation (MRDR) is created by rotation of the MCRR around axis perpendicular to  $z$  at angle  $\pi$ . The transmission function  $f(\gamma)$  of the MCRR is defined toward the radial axis crossing the dead point of the mechanism. It should be symmetrical and odd ( $f(-\gamma) = f(\gamma)$ ) where  $\gamma$  is the angle of rotation along the axis  $z$ . The profile of the wave could be any function satisfying the requirement for oddness toward the radial axis ( $x$  or  $y$ ). It gives the possibility to change the polar sinusoid into an other function in order to achieve non sinusoidal movement of the balls (for eliminating the change of the inertial force of the ball versus radius at fast rotation).

Two MCRR with phase shift of  $\pi/2$  are necessary for obtaining smooth rotation of a Mechanism for Reversing the Direction of Rotation (MRDR).

For statical and dynamical balance of the differential and in order to simplify the design, 4 identical MRDR each two of them with phase shift of  $\pi$  are used. It yields better torque transmission because the torque is transmitted by minimum two couples of balls. It assures also the static and dynamic balance of the differential, when the balls situated along the two perpendicular axes  $x$  and  $y$  are moving in opposite directions. It means that the balls in the perpendicular groves are moving with phase shift of  $\pi/2$ , or within a quarter of the cycle the number of the half waves is odd. The possible number  $i = (1, 3, 5, \dots)k/2$  gives for  $k = 4$ , the numbers  $i = 2, 6, 10 \dots$

The number of waves in the groves is also chosen according to the maximal allowed contact pressure between the ball and the groves. The smaller the number of waves is, the more sensitive the differential would be, but the maximum allowed torque also would be smaller. On the other hand, the bigger number of waves causes the ball to oscillate more times per turn. The sliding velocity of the ball is restricted by the properties of the materials and of the lubricant. In the model the groves in the disks have 6 waves for 1 turn.

According to [8] the transmission ratio between the balance link and the outputs is defining the type of the differential. If the force transmission ratio of the MCRR in direction from the wheel to the balance link is lower than the coefficient of friction, the MCRR behaves as a one-way blocking mechanism. In this case no power between the wheels could be transmitted through the second degree of freedom, because the

power transmitted by each of the MCRR's to the balance link is with opposite signs. The wheels could rotate at different speeds biasing the input moment when the reactive moments of the wheels are bigger than the moment of inner friction of the MCRR.

In order to obtain of the transmission ratio, the static forces acting on the differential are analyzed below.

#### 4. Static forces acting on the elements of the differential

A schema of the driving separator with 4 windows which transmits the moment  $M_{ab}$  to the balls is shown in Fig.3. The balls divided the moment equally over the the two output disks through the sinusoidal grooves.

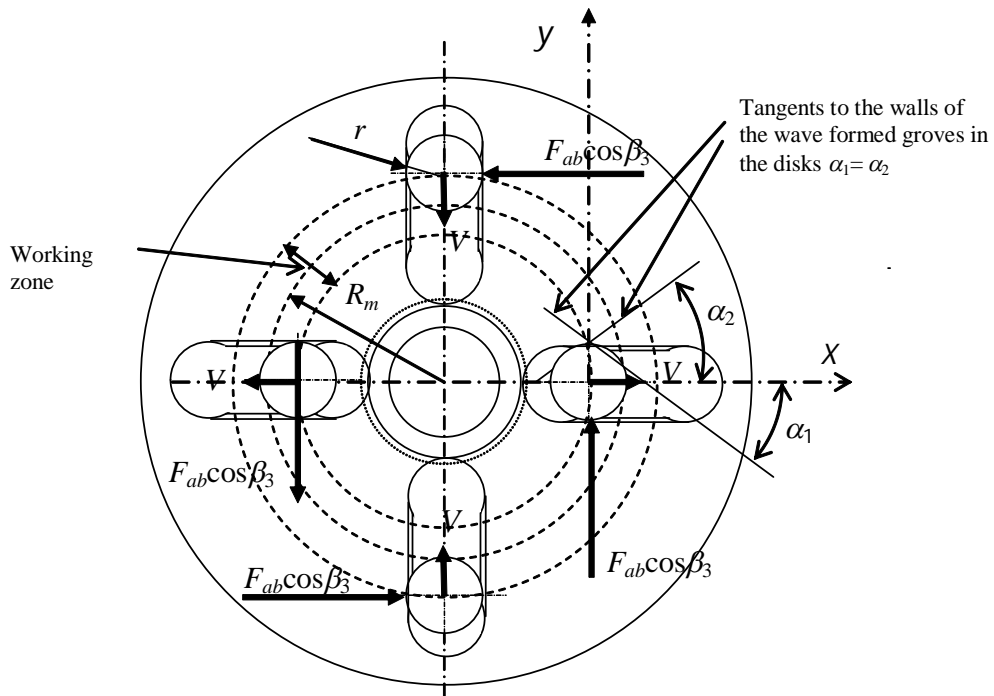


Fig. 3. Schema of the force transmission between the driving separator and the balls

The force  $F_{ab} \cos \beta_3$  is

$$(1) \quad F_{ab} \cos \beta_3 = \frac{\eta M_{ab}}{k R_m}.$$

For the reaction moments  $M_a$  and  $M_b$  is yielded:

$$(2) \quad \eta M_a = k R_m F_a \cos \beta_1 \cos \alpha_1,$$

$$(3) \quad \eta M_b = k R_m F_b \cos \beta_2 \cos \alpha_2.$$

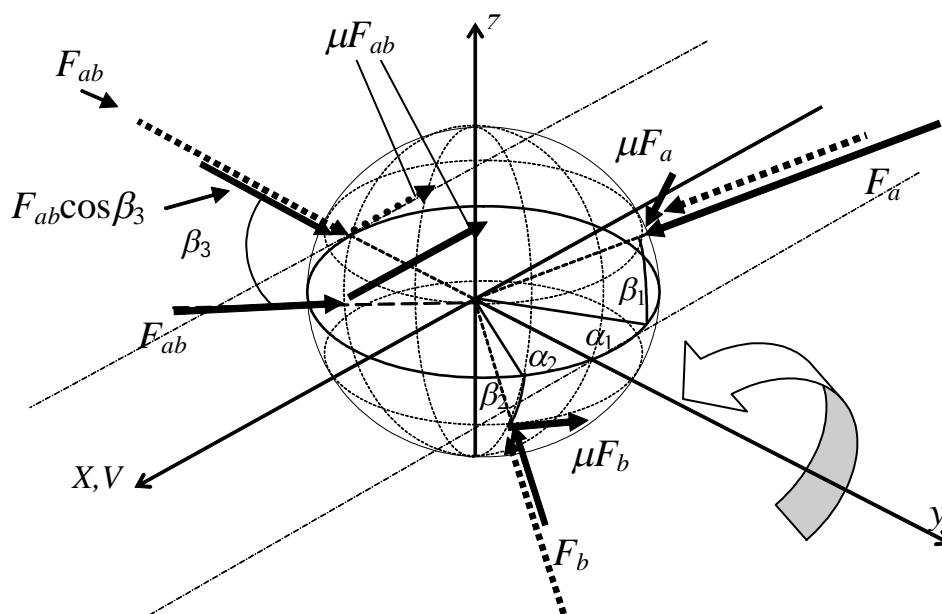


Fig. 4. Schema of the forces acting on one ball. The forces  $F_a$ ,  $F_b$  and  $F_{ab}$  at equal reactive torques (no slip,  $\beta_3=0$ ) are shown with dashed lines. The forces at low  $M_b$  – with continuous line. The arrow shows the direction of rolling of the ball under the couple of forces  $\mu F_a$  and  $\mu F_b$

On Fig. 5 the average axial play  $\delta$  and the possible movement between the balls, and the grooves under the forces  $F_a$  are shown.

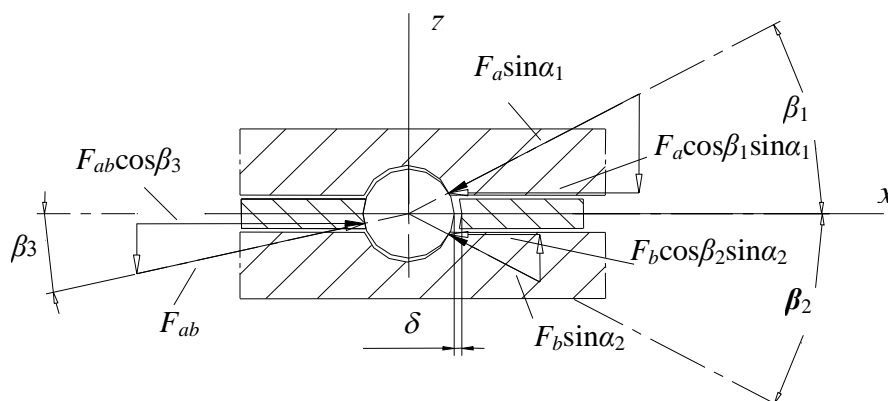


Fig. 5. Projection of the forces acting on the ball and the grooves of the separator and the disks on the plane  $yOz$

## 5. Geometrical relations

The equation of the axis of the wave formed groove in polar coordinates is described by the average radius of the grooves into the disks, the amplitude of the axis of the grooves and the number of the waves of the grooves:

$$(4) \quad \rho = R_m + d \cos k\varphi,$$

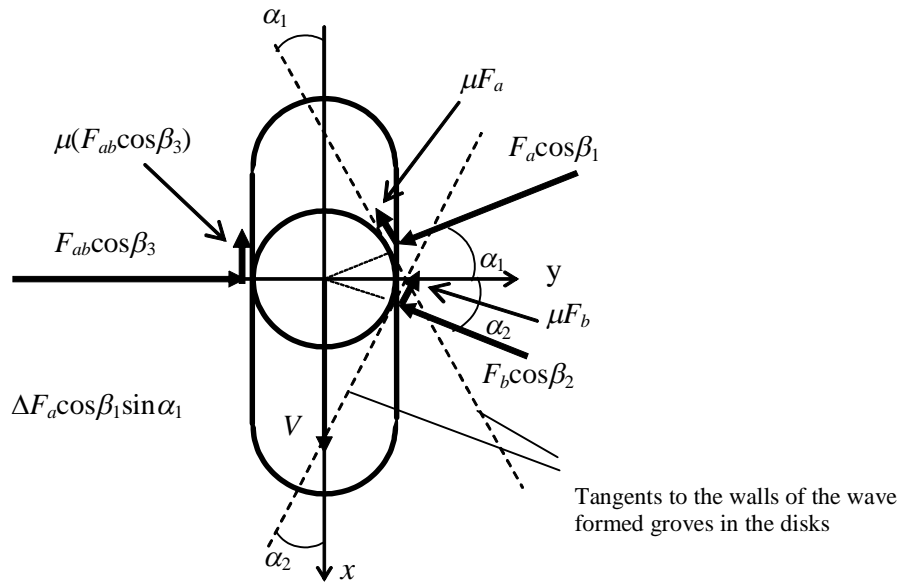


Fig. 6. Projection of the forces acting on the ball on the plane  $xOy$

where  $\rho$  is the radius vector of the curve,  $\varphi$  – polar angle.

The angle between the tangent to the axis of the curved groove and the radius vector is:

$$(5) \quad \alpha = \arctg \frac{\rho}{\rho'_{\varphi}} = \arctg \frac{R_m + d \cos k\varphi}{-k d \sin k\varphi}$$

The curve of the radius vector  $\rho$  and the variation of  $\alpha$  as function of angle  $\varphi$  are shown in Fig. 7.

The equilibrium equations on the ball in the working zone (Figs. 4, 5 and 6) are:

$$(6) \quad \sum x_i = 0, F_a \cos \beta_1 \sin \alpha_1 + \mu F_a \cos \alpha_1 - F_b \cos \beta_2 \sin \alpha_2 + \mu F_b \cos \alpha_2 - \mu F_{ab} = 0;$$

$$(7) \quad \sum y_i = 0, F_{ab} \cos \beta_3 + \mu F_b \sin \alpha_2 - \mu F_a \sin \alpha_1 - F_a \cos \beta_1 \cos \alpha_1 - F_b \cos \beta_2 \cos \alpha_2 = 0;$$

$$(8) \quad \sum z_i = 0, F_{ab} \sin \beta_3 - F_a \sin \beta_1 \cos \alpha_1 + F_b \sin \beta_2 \cos \alpha_2 = 0;$$

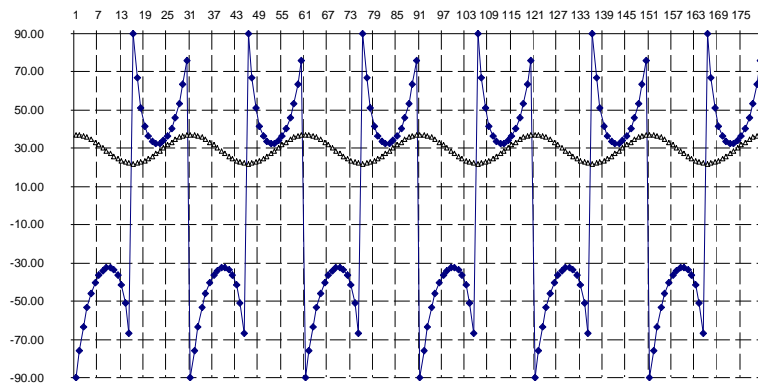


Fig. 7. Curve of the variation of the angle  $\alpha$  trough length of the wave formed groove according to equation (5) for parameters:  $i = 6$ ,  $k = 4$ ,  $d = 7.5$  mm and  $R_m = 29.5$  mm

$$(9) \quad \sum M_{ix} = 0, \quad \mu F_a \cos \alpha_1 r \sin \beta_1 - \mu F_b \cos \alpha_2 r \sin \beta_2 = 0;$$

$$(10) \quad \sum M_{iy} = 0, \quad \mu F_a \sin \alpha_1 r \sin \beta_1 - \mu F_b \sin \alpha_2 r \sin \beta_2 + \mu F_{ab} r \sin \beta_3 = 0;$$

$$(11) \quad \sum M_{iz} = 0, \quad \mu F_{ab} r \cos \beta_3 - \mu F_a r \cos \beta_1 - \mu F_b r \cos \beta_2 = 0;$$

the forces  $F_i$  and angles  $\alpha_i$  and  $\beta_i$  are obtained from equations (1)-(11). For the considered mechanism  $\alpha_1 = \alpha_2 = \alpha$ .

For preliminary calculations the angle  $\beta$  can be obtained from the thickness of the wall of the separator  $h$  and the radius of the ball  $r$ :

$$(12) \quad \beta = \arcsin(h/r).$$

## 6. Behavior of the differential at different working conditions

The difference of the torque on the tires (caused by the ground at turns) drives the second DOF (overcoming the torque of inner friction) in order to balance the driving torque on the tires. So the torque biasing accuracy depends on the inner friction through the second DOF.

At different velocities but at equal reactive torque (no slip) on the two tires, the balls reciprocate into the groves dividing the input torque. The ball slides along the groove in the separator, with the friction force  $\mu F_{ab}$  and simultaneously rolls along the wave formed groves in the output disks under the couple of friction forces  $\mu F_a$  and  $\mu F_b$  (fig. 4). The error of dividing of the input torque is equal to the torque of friction forces between the balls and the walls of the separator. The torque biasing accuracy of the differential is  $2M_f$  :

$$(13) \quad M_a = M_b \pm M_f,$$

where  $M_f = 4R_m \mu F_{ab}$ , is the torque caused by the friction force between the wall of the separator groves and the balls.

$$(14) \quad F_a = F_b \pm \mu F_{ab}.$$

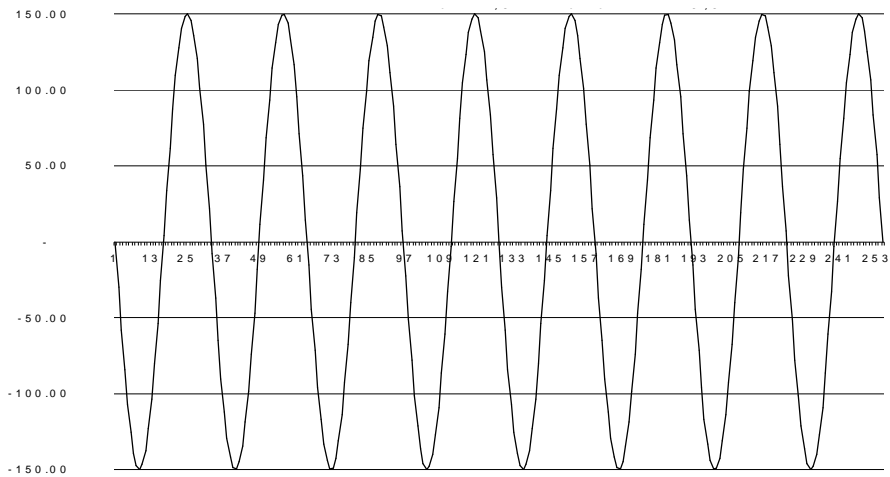


Fig. 8. Velocity of the balls in (mm/s) at  $\Delta n = 200$  1/s for parameters:  $i = 6$ ,  $k = 4$ ,  $d = 7.5$  mm and  $R_m = 29.5$  mm



When the reactive torques on the tires differ (one tire on ice), a difference of the forces over the ball arises (Fig. 4). Under the action of these forces, the ball moves towards the groove of the output disk with the lower reactive moment. This causes a significant increasing of the force  $F_{ab}$  and the friction force  $\mu F_{ab}$ . The bigger difference causes a bigger friction force that resists the torque biasing, the ball rolling stops and this causes blocking of the differential. The differential blocking ends when the reactive torques become equal again:  $M_a = M_b$ .

## 7. Conclusion

Some basic dependences necessary for the preliminarily design of the differential are obtained in the paper. The principle of the blocking of the differential when the reactive torques differ is described. This work should continue with experimental research and investigation of the dynamics of the differential at different working conditions.

## References

1. J a s k e v i c h, Z. Leading Bridges. Machine Building, 1985 (in Russian).
2. L o o m a n, J. Zahnradgetriebe. Berlin-Heidelberg-New York, Springer Verlag, 1996.
3. M a d h a v a n, B., L - W. T s a i. T.R.96-42. Technical Research Report. Systematic Enumeration of 1:-1 Constant-Velocity Couplings. 1996.
4. S t a i n o v, G. S. Differential Pat, No BG 62 788 F16H48/12, 1998 (in Bulgarian).
5. S t a i n o v, G. S. Design of a Spherical Differential Mechanism. – Scientific Reports of the Sc. – Techn. Union of Machine Building, 1998, 1.1-1.11 (in Bulgarian).
6. S t a i n o v, G. S. Differential Mechanisms in Which the Rotating Movement is Transformed in Reciprocating. – Scientific Reports of the Sc. – Techn. Union of Machine Building, 2000, 3,1-3.10 (in Bulgarian).
7. S t a i n o v, G. S. Design of symmetrical differential mechanisms. – Scientific Reports of the Sc.-Techn. Union of Machine Building, 2001, 2.77-2.83 (in Bulgarian).
8. S t a i n o v, G. S. Differentials with Limited Sliding – Analysis and Computation. – Scientific Reports of the Sc.-Techn. Union of Machine Building, 2001, 2.73-2.77 (in Bulgarian).
9. M i m u r a K e n j i. Differential Gear. Patent number: US5577423 (1996), Int.Cl. F16H35/04C.

## Теоретическое исследование дифференциала без зубчатых колес

*Генчо Стайнов*

*Центральная лаборатория мехатроники и приборостроения, 1113 София*

*E-mail: gentcho@clmi.bas.bg*

### (Р е з ю м е)

В статье представлен новый дифференциал без зубчатых колес. Сделан анализ дифференциала согласно специфически для этих механизмов критерии. Исследованы теоретические зависимости для сил и скоростей скольжения балансных звеньев во время работы дифференциала. Полученные уравнения позволяют сделать предварительное вычисление дифференциала для данного крутящего момента. Исследовано поведение механизма для разных рабочих режимов. Показано, что аксиальная хлабина балансного звена делает механизм чувствительным к различию реактивных крутящих моментов: увеличение разницы между реактивными моментами колес причиняют повышение внутреннего трения до полного застопорения.